The influence of the timing of Sudden Stratospheric Warmings on precipitation anomalies in Europe

Erika Monnin[1], Marlene Kretschmer[2,*], Inna Polichtchouk[3]

[1] ENSTA Paris, Palaiseau, France

[2] Department of Meteorology, University of Reading, Reading, UK

[3] European Centre for Medium-Range Weather Forecasts, Shinfield Rd, Reading RG2 9AX, UK

*corresponding author, m.j.a.kretschmer@reading.ac.uk (@Marlene_Climate)

THIS IS A NON-PEER REVIEWED PREPRINT SUBMITTED TO EARTHARXIV. THE MANUSCRIPT HAS BEEN SUBMITTED FOR PEER REVIEW TO THE *INTERNATIONAL JOURNAL OF CLIMATOLOGY*.

Abstract

The Northern Hemisphere stratospheric polar vortex (SPV), a band of fast westerly winds over the pole extending from approximately 10 to 50 km altitude, is a key driver of European winter weather. Extremely weak polar vortex states, so called sudden stratospheric warmings (SSW), are on average followed by dry and cold weather in Northern Europe, as well as wetter and warmer conditions in Southern Europe. However, the surface response of SSWs varies greatly between events, and it is not well understood which factors modulate this difference. Here we address the role of the timing of SSWs within the cold season (December to March) for the precipitation response in Europe. Due to the limited sample size of SSWs in the observational record, hindcasts of the seasonal forecasting model SEAS5 from the European Centre for Medium-Range Weather Forecasts (ECMWF) are analysed. We first evaluate key characteristics of stratosphere-troposphere coupling in SEAS5 against reanalysis data and find them to be reasonably well captured by the model, justifying our approach. We then show that in SEAS5, early winter (December and January) SSWs are followed by more pronounced tropospheric zonal wind and precipitation anomalies compared to late winter (February and March) SSWs. For example, in Scotland the low precipitation anomalies are roughly twice as severe after early winter SSWs than after late winter SSWs. The difference in the response cannot be explained by more downward propagating SSWs in early winter, or by different monthly precipitation climatologies. The role of SSW timing is potentially of use for forecasts and early warnings of European weather on sub-seasonal to seasonal timescales.

1 Introduction

Skilful forecasts of European winter weather are of great importance for several weather-dependent sectors, such as the health (Charlton-Perez *et al.*, 2021) or renewable energy sector (Van Der Wiel *et al.*, 2019; Büeler *et al.*, 2020) allowing them to prepare and to take early actions. However, predictions on sub-seasonal to seasonal (S2S) timescales, i.e. predictions beyond the typical weather prediction time-scale of 10 days and up to a season ahead, remain difficult due to the complex and chaotic nature of the climate system (Weisheimer and Palmer, 2014; White *et al.*, 2017; Vitart and Robertson, 2018). To make progress, an improved understanding of the different physical drivers affecting winter weather is necessary (Mariotti *et al.*, 2020).

One known driver of European weather on S2S timescales is the Northern hemisphere stratospheric polar vortex (SPV) (Baldwin and Dunkerton, 2001; Kretschmer *et al.*, 2018a, 2018c; King *et al.*, 2019; Domeisen and Butler, 2020). The SPV is a band of strong westerly winds in the Arctic stratosphere which forms during boreal autumn (Waugh *et al.*, 2016). It stems from a strong temperature gradient between the Arctic and the lower latitudes due to the lack of incoming solar radiation over the Arctic during the cold season, and it breaks down again in spring when sunlight returns to the pole. Extreme weak phases of the SPV, such as major sudden stratospheric warmings (SSW), during which the vortex breaks down and the winds in the stratosphere reverse, can affect the tropospheric circulation below (Baldwin and Dunkerton, 2001; Waugh *et al.*, 2016). In particular, SSWs are often followed by persistent negative phases of the North Atlantic Oscillation (NAO-) and the associated weather patterns. For instance, in the weeks after SSWs there is usually increased precipitation over Southern Europe while Northern Europe experiences more cold and dry weather conditions (Beerli and Grams, 2019; King *et al.*, 2019).

The observed average effects of SSWs for Europe are well documented (Ayarzagüena *et al.*, 2018; Kretschmer *et al.*, 2018a; King *et al.*, 2019; Afargan-Gerstman and Domeisen, 2020; Kautz *et al.*, 2020) but the surface impacts vary strongly across events. Only roughly half of the observed SSWs have been classified as downward-propagating events, meaning that the stratospheric anomalies were followed by the canonical NAO- response in the troposphere (Karpechko *et al.*, 2017). For the other events, so-called non-downward propagating SSWs, the stratospheric circulation anomalies were mostly confined to the stratosphere. As the exact downward coupling mechanisms of SSWs are not understood (e.g. Hitchcock and Simpson, 2014) it is also not clear which factors modulate this difference.

To better understand the variability in the surface response of SSWs, several previous studies classified SSWs according to different event characteristics. For example, SSWs have been distinguished by their horizontal spatial structure (vortex split vs vortex displacement events), although no strong differences

in the tropospheric circulation response were found when analysing a large set of events in a climate model (Maycock and Hitchcock, 2015). Moreover, differences in the troposphere-stratosphere coupling mechanism have been addressed (absorptive vs reflective events), with the absorbing-type events in particular being associated with downward-propagating SSWs and the canonical NAO-surface response (Kodera *et al.*, 2016; Kretschmer *et al.*, 2018a; Matthias and Kretschmer, 2020). Recent studies also tackled the importance of the prevailing North Atlantic weather regime during the occurrence of SSWs and addressed how this modulates the surface response (Beerli and Grams, 2019; Domeisen *et al.*, 2020). For example, Domeisen et al. (2020) found that high pressure anomalies over Greenland (which project onto NAO-) are more likely to happen when the regime during the SSW onset is a European Blocking regime (negative pressure anomalies over western Europe). Overall, several factors likely contribute to the surface response, but which and how exactly remains an open question.

The purpose of this study is to investigate whether the *timing* of a SSW within the cold season (from December to March) plays a role in the surface response. While SSWs are linked to a range of extreme events in different regions (Domeisen and Butler, 2020), here we focus on anomalous precipitation in Europe. Due to the limited observational record we make use of the large-ensemble hindcasts SEAS5 of the seasonal prediction model from the European Centre for Medium-Range Weather Forecasts (ECMWF), which provides a much larger sample of SSWs and allows us to address our research question with statistical confidence (Stockdale *et al.*, 2018; Johnson *et al.*, 2019).

2 Data and methods

2.1 Data

We use the ERA5 reanalysis dataset provided by ECMWF as observations (Hersbach *et al.*, 2020). We use daily mean data from November 1981 to May 2019. The zonal wind velocity at 10 hPa is used to detect SSWs, and the zonal wind velocity at 850 hPa as well as total precipitation is used to describe their surface impacts. Moreover, geopotential height data at 1000 hPa and 150 hPa is used to study the downward propagation of SSWs.

Given the incomplete sampling of SSWs in the observations, output of the same variables from ECMWF's seasonal forecasting model SEAS5 is further used (Stockdale *et al.*, 2018). Details of the model configurations are described in Johnson et al. (2019). We use the 12-hourly output within the extended winter season (November to April) from the re-forecasts initialized on the 1st of November of each year from 1981 to 2018, from which we form daily means. The dataset contains 51 ensemble members, thus providing 51 times more data over the same time period as compared to the

observations. In our analyses, we focus on the SEAS5 output from December onward, such that the initial conditions play a minor role.

For all data, climatological anomalies are constructed by first removing the multi-year mean of each day. For SEAS5 data, the multi-year mean over all ensemble members is subtracted. Note that the multi-year mean is calculated for days of the same forecast lead-time relative to the initialization date, resulting thus in 1-day shifted calendar days in March in leap years. The ERA5 dataset is interpolated from a native T639 grid onto the 0.25° latitude and 0.25° longitude grid. The SEAS5 precipitation data is interpolated from a native TCo319 grid onto a 1° latitude and 1° longitude grid, and the wind and geopotential height data is interpolated onto a 2.5° latitude and 2.5° longitude grid.

2.2 Methods

We use the commonly applied definition of Charlton and Polvani (2007) to define SSWs. Accordingly, a SSW is detected when the zonal-mean zonal wind at 60°N at 10 hPa from November to March is negative, i.e. the zonal-mean zonal wind is easterly (Charlton and Polvani, 2007). The first day this value becomes negative is called the central date of the SSW. This definition further requires that no other SSW is detected for at least 20 days after the winds have become positive again. This way, even if the winds become westerly for a few days, the same event is not counted twice. Finally, the definition requires that the zonal mean zonal wind must return to positive for at least 10 consecutive days before April 30th to ensure that SSWs are not mistaken for the final warming of the polar vortex.

To describe the downward coupling of SSWs to the troposphere, the Northern Annular Mode (NAM) index is used (Karpechko *et al.*, 2017; White *et al.*, 2019). The NAM is calculated following Karpechko et al. (2017) as the area-weighted average of daily mean geopotential height over the polar cap (60-90°N) for a given pressure level. Next, the index is standardized by subtracting the multi-year climatology of each day and dividing it by the daily multi-year standard deviation.

This standardized NAM index is then used to classify SSWs into downward (dSSW) and non-downward (nSSW) propagating events. Downward propagating events are those SSWs that fulfil the three following criteria: (1) the 1000 hPa NAM index (NAM1000) averaged over the 8 to 53 days after the SSW central date must be negative, (2) at least 50% of all days within this 8 to 53 period must have a negative NAM1000 value, (3) at least 70% of days within the 8 to 53 period must have a negative NAM150 value. Note that for the third criteria we used the 150 hPa instead of the 100 hPa pressure level that was used in Karpechko et al. (2017), as the latter is not part of the SEAS5 output. According to White et al. (2019) the use of 150 hPa leads to similar results.

To address the role of sampling uncertainty, we use a bootstrap approach following Byrne et al. (2019). We generate 10,000 timeseries of length 38 years by randomly selecting one of the 51 ensemble members for each year. From these 10,000 timeseries we then create a distribution of the studied characteristics (e.g. the number of SSWs per winter month) and compare the observations to it (Byrne *et al.*, 2019).

3 Results

3.1 Model evaluation

To first evaluate how well SEAS5 is capable of simulating the SPV and its variability, we compare its key characteristics in the reanalysis with that of SEAS5. The SPV strength is here defined as the zonal-mean zonal wind velocity at 60°N at 10 hPa. Fig. 1a shows the climatology (black thin line) as well as one and two standard deviations (grey shadings) of the SPV over the course of the extended winter season. Strong westerly winds are observed during the winter that peak in January when vortex variability is also the largest. The winds then progressively slow down until turning on average negative in April. Similar characteristics can be seen in the SEAS5 model, overall giving a smoothed picture due to the larger number of data (Fig. 1b). In contrast to ERA5, the climatological wind is strongest in December in the model.

We next calculate the number of SSWs per winter in both ERA5 and SEAS5 (Fig. 1c). In total 27 SSWs occurred during the 38 considered winters from November 1981 to April 2019 in the observational record, giving an average occurrence of 0.71 SSWs per winter. These events contain the same dates as the list of 23 major SSWs provided in Karpechko et al. (2017) based on Era-Interim data, with two additional events found on 17 February 2002 and 29 March 2008 in the ERA5 data set used here, as well as on 20 March 2018 and 1 January 2019, which occurred after the above study was published. In contrast, the 51 SEAS5 ensemble members contained 1705 events, giving an average of 0.88 SSWs per winter.

To understand the role of sampling variability in Fig.1 a-c, we next follow a bootstrap approach to create a distribution of 10,000 time-series of length 38 years from the model ensemble and compare the observations to it (see also Methods). We compute the mean (Fig. 1d) and the standard deviation (Fig. 1e) of the SPV index over the course of the winter. The mean over all values is shown by the thin black line, while that of the observations is indicated in red. The grey shadings indicate the 1%, 5%, 25%, 75%, 95% and 99% percentile thresholds. While observed SPV variability (red line in Fig. 1e) is well within sampling uncertainty, the SPV mean in January lays outside the model spread (red line in

Fig. 1d), suggesting that the mean strength is underestimated by the model during this time. Additional analysis showed that this bias was not present in the SEAS5 data initialized on the 1st of December (not shown). Moreover, we also compute the frequency of SSWs for all timeseries and show them in a box and whiskers plot with the observations again indicated in red (Fig. 1f). Although the SSW frequency was found to be lower in the observations (Fig. 1c), it is still consistent with sampling uncertainty. We further note that the weak bias in the model in January (Fig. 1d) might contribute to the higher number of SSWs per winter in SEAS5, since their detection depends on the absolute threshold of 0 m/s. Overall, Fig. 1 shows that despite these small differences, the SPV seasonal evolution and variability, including SSW frequency, are well captured by SEAS5.

Next, we compare the surface impacts following SSWs in the model and the observations (Fig. 2). We do this by plotting the zonal wind velocity anomalies at 850 hPa (u850, Fig. 2a and 2b) and the precipitation anomalies (Fig. 2c and 2d) averaged over the 30 days after the central date of all detected SSWs in the observations (Fig. 2a and 2c) and in SEAS5 (Fig. 2b and 2d). The observations show the expected negative NAO-type response. There are negative wind anomalies over the North Atlantic and Scandinavia while wind anomalies over Southern Europe are positive (Fig. 2a). This indicates southward shifted Atlantic storm tracks, transporting moist air to Southern Europe. Consistently, precipitation anomalies over Southern and Central Europe are anomalously high (Fig. 2c). In particular, the Iberian Peninsula as well as Italy and the Balkan region show increased precipitation. In contrast, precipitation over Iceland, Ireland, Scotland and Norway is on average anomalously low in the months after a SSW. Similar patterns are found in SEAS5 (Fig. 2b, d). While negative wind anomalies over the North Atlantic following SSWs are more pronounced in the model (Fig. 2b), associated precipitation anomalies are less extreme in SEAS5 (Fig. 2d). The latter might at least partly be related to the higher numbers of events in the model compared to the observations, which will tend to blur the effects of individual events.

In summary, Fig. 1 and Fig. 2 show that SEAS5 depicts polar vortex variability and the surface weather impacts following SSWs reasonably well. This justifies our approach to use the SEAS5 model data to study the role of SSW timing on precipitation impacts over Europe.

3.2 The role of SSW timing on the surface response

To investigate the role of the SSW timing on European precipitation, we first study the monthly distribution of the frequency of SSWs. Fig. 3a shows the percentage of SSWs that occurred in a given winter month, both for ERA5 (in red) and SEAS5 (in blue). We observe that SSWs are more likely to occur in January and February (27% and 38% of all events) and less likely to occur in December and

March (13% and 20% of all events) both in the observations and in SEAS5. Unlike the observations, the model contains a few events in November which we ignore in the following.

As before, the role of sampling uncertainty on the monthly occurrence rates is studied using a bootstrap approach. Fig 3b shows the number of SSWs per month per winter in the 10,000 timeseries using box and whiskers plots, with the observations indicated in red. On average, there are as many SSWs in January as in February, and as many in December as in March, with the latter group having much lower numbers of events than the former, consistent with Fig. 3a. Furthermore, we note that the observations lie in the second quartile in December, February and March, and a little bit below in January. Thus, the differences between the model and the observations are again consistent with sampling variability.

Similar to Fig. 2b, d, we next plot the u850 and precipitation anomalies in SEAS5, averaged over the 30 days after the SSW central date, this time separately for each month of SSW occurrence (Fig. 4). The canonical negative NAO-type response is found for each month. That is, there are on average windier and wetter weather conditions in Southern Europe, while Northern Europe experiences less wind and rain. Interestingly, the strength of the anomalies is weakening as the winter season progresses. While early winter (December and January, DJ) events are followed by strong u850 and precipitation anomalies, the response is less pronounced in late winter (February and March, FM). For example, while average precipitation anomalies over the Balkans in the month after a SSW occurring in December exceed 1 mm/d, they are close to climatology after March SSWs. Similarly, rainfall is strongly decreased over Scotland after early winter SSWs, while the signal is only weak after late winter events.

To investigate the difference between early and late winter SSWs in more detail, we compute regional indices of precipitation anomalies for four regions particularly affected by SSWs (see Fig. 5a). We follow King et al. (2019) and consider precipitation anomalies in Iberia and Eastern Europe (which are both associated with anomalously high precipitation after SSWs), as well as over Scotland and Norway (which are both associated with anomalously low precipitation after SSWs). Note that the latter two regions are smaller than the regions considered by King et al. (2019). Figure 5b shows the 30 day-average following SSWs for each region and month, normalised by the multi-year average of the month of the central date of the SSWs. That is, precipitation anomalies following SSWs occurring in December are divided by the December precipitation climatology, etc. Consistent with Fig. 4, the regional anomalies following SSWs - now expressed as percentages of the monthly climatology - decrease over the course of the winter. For example, after SSWs occurring in December there is on average 17% more precipitation in Iberia and 15% in Eastern Europe, compared to their December climatology. In contrast, SSWs occurring in March only show an increase in 8.7% and 2.4% respectively of the

climatology of that month. Similarly, the anomalously low precipitation in Scotland and Norway decreases from 5.5% and 12% after December SSWs to just 1.5% respectively 3.6% after SSWs occurring in March. This means, in particular, that the results from Fig. 4 are not the result of overall lower precipitation climatologies in late winter. These findings are also robust (not shown) when normalising the precipitation anomalies by the 15 days shifted monthly average (i.e., calculated from the 15th of the month of the central date up to the 15th of the following month), to account for the fact that precipitation composites following SSWs also include days outside of the month of the central date.

We next test how these findings compare to the observations, including whether the results are consistent within sampling variability using a bootstrap approach. Figure 6 shows the observed precipitation anomalies (expressed as percentages) in the four different regions after early (DJ, dark blue bars) and late winter (FM, yellow bars) SSWs. We reduce our analysis to early and late winter events here, to increase the analysed sample size of the observations. Except for Iberia, precipitation anomalies in ERA5 are more pronounced after early winter SSWs, consistent with Fig. 4 and 5. Given the noise in the observations, some inconsistency is to be expected. We further address this by showing the median precipitation anomaly for the 10,000 time-series in SEAS5 (light blue and orange bars), with the black lines indicating the 5th and 95th confidence interval. While observed results for Scotland, Norway and Eastern Europe, as well as early winter results for Iberia are well within sampling variability, the late winter SSW response for Iberia is not. Note, however, that the confidence interval is widest for this region, indicating that sampling variability can at least contribute to this difference. For Scotland and Norway, observed differences between early and late winter SSWs are even more pronounced than in the model. Overall, despite the outlier of Iberian precipitation after late winter SSWs, the observed precipitation response following early and late winter SSWs is mostly consistent with SEAS5. Recall that the confidence intervals are on the subsamples representative of the observations, just as in Figs. 1d,e and Fig 3b. This means that the observations on their own cannot be definitive for any particular region or half-winter period, but they are consistent with the behaviour we see in the model.

3.3 Are there more downward propagating SSWs in early winter?

Next, we investigate a potential dynamical explanation for this difference between the early and late winter SSW response. More precisely, we test if there are more SSWs that are downward propagating to the troposphere in early winter than in late winter. This could explain the more pronounced surface response in early winter, as downward propagating SSWs show by definition a stronger response in

the tropospheric circulation (Karpechko *et al.*, 2017). To test this hypothesis, we categorize each SSW into either downward propagating (dSSWs) or non-downward propagating SSWs (nSSWs) (see also Methods). We then first evaluate how well these properties are captured by the model. To do this we plot the monthly share of dSSWs for both ERA5 and SEAS5 (see dashed line in Fig. 7a) and again address the role of sampling uncertainty of this ratio using a bootstrap approach as before (Fig. 7b). We make two observations.

Firstly, we find that there are more dSSWs in the observations than in SEAS5. In Fig. 7a only half of January and February SSWs are downward propagating in the model, while more than 80% of those in the observations are dSSWs. In contrast, the share of dSSWs in December in the model is twice as large as that in the observations. Furthermore, there are some detected dSSWs in March in SEAS5 while there are none in ERA5. The box and whiskers plots in Fig. 7b show that these rather strong differences are yet still consistent with sampling uncertainty, albeit being on the outer edges of the distributions.

Secondly, Fig. 7a shows that there is no clear difference in the number of dSSWs occurring in early and late winter. In fact, the percentage of dSSWs in early winter (24% of all events) is approximately the same as in late winter (20%). Thus, the ratio of dSSWs cannot explain the difference between the early (DJ) and late winter (FM) SSW responses shown in Fig. 4. To confirm this, we also plot the precipitation anomalies in the 30 days following only the dSSWs for each month of the winter period (Fig. 7c). By construction, the precipitation anomalies are now much more pronounced, as only the stratospheric events that reach the troposphere are included. However, we still find that the anomalies are weaker after late winter SSWs. This confirms a role of the timing of SSWs for their precipitation response that cannot be explained by different numbers of downward-propagating SSW events.

3.4 Regional risk of extreme events

Finally, we address how the timing of SSWs is related to the occurrence of extreme events. For consistency with the previous results, we again analyse the 30 days averaged precipitation anomalies after SSWs. Fig. 8 shows the probability density function of such precipitation anomalies for early winter (blue) and late winter (orange) SSWs. The respective means are indicated by the dashed lines and extreme percentiles (10% for the British Isles and Southern Scandinavia, 90% for Iberia and Eastern Europe) are shown by the dotted lines. Clearly, not only is the mean precipitation shifted in all regions, coherent with our previous findings (Fig. 4, 5), but also the extreme values are more pronounced in each region after early winter SSWs. These results are also consistent with those of King et al. (2019) for the observations.

To better quantify the risk of extreme events following early and late winter SSWs, we further compute the risk ratios for each region. In order to do so, we computed the top and bottom 10% extreme 30-day averaged precipitation anomalies for each region. The risk ratio is the probability of an extreme event occurring after the central date of an early winter SSWs, divided by the probability of it occurring after late winter SSWs. Here we find risk ratios of extremely low precipitation (below the 10th percentile) of 1.7 Scotland and of 2.6 for Norway. This means, for example, that the risk of extremely dry conditions is more than doubled in Norway after the occurrence of an early winter SSW compared to that of a late winter SSW. Consistently, we find risk ratios of extremely high precipitation (above the 90th percentile) of 1.7 both for Iberia and for Eastern Europe. Thus, consistent with the previous analysis, the risk of extreme anomalous precipitation is roughly increased by a factor of two after early winter SSWs compared to that of late winter SSWs.

4 Discussion

Our results suggest that the timing of SSWs plays an important role for their surface impacts, with early winter SSWs being followed on average by stronger precipitation anomalies compared to late winter SSWs. Overall, this study thus contributes to a larger body of literature arguing that seasonal-mean analyses of teleconnections, and of stratosphere-troposphere coupling in particular, can blur over important details (Jiménez-Esteve and Domeisen, 2018; Kretschmer *et al.*, 2018b; King *et al.*, 2021). The reasons behind the role of SSW timing for the severity of the precipitation anomalies remains unclear. Here we tested if the number of downward propagating SSWs can explain the different precipitation anomalies, but found this not to be the case. Similarly, the seasonal evolution of climatological precipitation cannot explain the differences. Hence, other potential drivers and mechanisms modulating the response need to be studied. For example, it is possible that the onset regimes during SSWs differ between early and late winter events. A next step could be to study the temporal distribution of weather regimes preceding SSW events (Beerli and Grams, 2019; Domeisen *et al.*, 2020). Moreover, other teleconnection patterns and their seasonal dependencies might give further insights. For example, the influence of La Niña on the NAO is mostly observed during February but not during the other winter months (Jiménez-Esteve and Domeisen, 2018). Similarly, other recent work suggests that the North Atlantic response to ENSO in late autumn is different compared to mid-winter (King *et al.*, 2021). Understanding how these other mechanisms are related with our findings is important but is beyond the scope of the present study.

The larger surface response for early winter SSWs begs the question of whether predictability of European weather is enhanced following early winter SSWs as opposed to following late winter SSWs. Thus,

a potential further step would be to analyse the change in European predictability in monthly large ensemble forecasts initialised during the central date of early winter and late winter SSWs. Moreover, understanding if surface impacts following strong polar vortex states (which are associated with a positive NAO-type response) are also dependent on their timing could be interesting. In this context, it is also important to assess how and if the timing of SSWs plays a role for surface impacts in other regions. Here we focused on precipitation in Europe, but it is well documented that SSWs also affect extreme events in other regions in the Northern Hemisphere (Domeisen and Butler, 2020). Comparing the response in other regions might also shed light on the reasons for the early and late winter differences.

Finally, we note that although we found SEAS5 to reasonably well represent SSW frequency and downward coupling characteristics, we cannot make direct inferences concerning the real world because of sampling limitations in the observed record. For example, model biases (Tietsche *et al.*, 2020), as e.g. in the SPV strength for January in SEAS5 might affect our results. The observed increased precipitation in Iberia after late winter SSWs was more pronounced than in the model but the reasons for that were not investigated here. Testing our findings in other models and for shorter lead-times, e.g. such as in models participating in the S2S project (Vitart and Robertson, 2018), is therefore an important next step to understand the role of the timing of SSWs in more detail.

5 Summary and Conclusions

Sudden Stratospheric Warmings (SSWs) strongly impact European winter weather. This study analysed the role played by the timing of SSWs within the winter season on the precipitation response over Europe. To address this question we capitalized on the large ensemble hindcasts of the ECMWF seasonal forecast model SEAS5 initialized on the 1st of November of each year, providing a bigger archive of SSWs.

We analysed how well the model captures key stratospheric characteristics such as mean stratospheric wind velocity and variability (Fig. 1), average frequency of SSWs (Fig. 3) as well as the number of downward propagating SSWs (Fig. 7a,b), and found the model to reasonably capture the expected properties, with differences with the observations being mostly within sampling uncertainty. Moreover, we tested how well the precipitation and zonal wind velocities at 850 hPa after SSWs in the model resembled those in the observations (Fig. 2). While there were some differences, in particular regarding the North Atlantic wind anomalies, overall we found the model to well represent the surface impacts related to SSWs.

The analysis of the timing in SEAS5 suggested a difference between early (DJ) and late (FM) winter events. We found that early winter SSWs have a stronger impact on European weather, with higher precipitation anomalies (Fig. 4, 5). In contrast, late winter events have a smaller influence on surface weather. For example, while precipitation after December SSWs in Norway is reduced by approximately 12% of the monthly climatology, a reduction of only 4% was found after SSWs occurring in March. Except for Iberia, these results are consistent with the observed response of SSWs, despite the limited sample size (Fig. 6). Consistently, the risk of extreme precipitation anomalies in the month after the occurrence of SSWs is increased after early winter SSWs (Fig. 8). Moreover, we showed that this difference between early and late winter events cannot simply be explained by a different number of downward propagating SSWs, which were here found to be similar for early and later winter (Fig. 7).

In summary, this study suggests that the timing of SSWs plays a role for their surface response. This information, which also needs to be tested in other subseasonal-to-seasonal forecast models, could be valuable in the context of prediction of severe winter weather. For example, once a SSW is forecasted to occur, the timing could reveal valuable information and be used as early warnings for the weather-impacted sectors.

Acknowledgments

We thank Ted Shepherd for useful feedback and discussions which helped to improve the manuscript.

Funding information

M.K. has received funding from the European Union's Horizon 2020 research and innovation programme under the Marie Skłodowska-Curie grant agreement (No 841902).

References

Afargan-Gerstman H, Domeisen DIV. 2020. Pacific Modulation of the North Atlantic Storm Track Response to Sudden Stratospheric Warming Events. *Geophysical Research Letters*. Blackwell Publishing Ltd, 47(2). https://doi.org/10.1029/2019GL085007.

Ayarzagüena B, Barriopedro D, Garrido-Perez JM, Abalos M, de la Cámara A, García-Herrera R, Calvo N, Ordóñez C. 2018. Stratospheric Connection to the Abrupt End of the 2016/2017 Iberian Drought. *Geophysical Research Letters*. Blackwell Publishing Ltd, 45(22): 12,639-12,646. https://doi.org/10.1029/2018GL079802.

Baldwin MP, Dunkerton TJ. 2001. Stratospheric harbingers of anomalous weather regimes. *Science (New York, N.Y.)*. American Association for the Advancement of Science, 294(5542): 581–4. https://doi.org/10.1126/science.1063315.

Beerli R, Grams CM. 2019. Stratospheric modulation of the large-scale circulation in the Atlantic–European region and its implications for surface weather events. *Quarterly Journal of the Royal Meteorological Society*. John Wiley and Sons Ltd, 145(725): 3732–3750. https://doi.org/10.1002/qj.3653.

Büeler D, Beerli R, Wernli H, Grams CM. 2020. Stratospheric influence on ECMWF sub-seasonal forecast skill for energy-industry-relevant surface weather in European countries. *Quarterly Journal of the Royal Meteorological Society*. John Wiley and Sons Ltd, 146(733): 3675–3694. https://doi.org/10.1002/qj.3866.

Byrne NJ, Shepherd TG, Polichtchouk I. 2019. Subseasonal-to-Seasonal Predictability of the Southern Hemisphere Eddy-Driven Jet During Austral Spring and Early Summer. *Journal of Geophysical Research: Atmospheres*. Blackwell Publishing Ltd, 124(13): 2018JD030173. https://doi.org/10.1029/2018JD030173.

Charlton AJ, Polvani LM. 2007. A New Look at Stratospheric Sudden Warmings. Part I: Climatology and Modeling Benchmarks. *Journal of Climate*, 20(3): 449–469. https://doi.org/10.1175/JCLI3996.1.

Charlton-Perez AJ, Huang WTK, Lee SH. 2021. Impact of sudden stratospheric warmings on United Kingdom mortality. *Atmospheric Science Letters*, 22(2). https://doi.org/10.1002/asl.1013.

Domeisen DI V., Butler AH. 2020. Stratospheric drivers of extreme events at the Earth's surface. *Communications Earth & Environment*. Springer Science and Business Media LLC, 1(1): 1–8. https://doi.org/10.1038/s43247-020-00060-z.

Domeisen DI V., Grams CM, Papritz L. 2020. The role of North Atlantic–European weather regimes in the surface impact of sudden stratospheric warming events. *Weather and Climate Dynamics*. Copernicus GmbH, 1(2): 373–388. https://doi.org/10.5194/wcd-1-373-2020.

Hersbach H, Bell B, Berrisford P, Hirahara S, Horányi A, Muñoz-Sabater J, Nicolas J, Peubey C, Radu R, Schepers D, Simmons A, Soci C, Abdalla S, Abellan X, Balsamo G, Bechtold P, Biavati G, Bidlot J, Bonavita M, Chiara G, Dahlgren P, Dee D, Diamantakis M, Dragani R, Flemming J, Forbes R, Fuentes M, Geer A, Haimberger L, Healy S, Hogan RJ, Hólm E, Janisková M, Keeley S, Laloyaux P, Lopez P, Lupu C, Radnoti G, Rosnay P, Rozum I, Vamborg F, Villaume S, Thépaut J. 2020. The ERA5 Global Reanalysis. *Quarterly Journal of the Royal Meteorological Society*. Wiley, qj.3803. https://doi.org/10.1002/qj.3803.

Hitchcock P, Simpson IR. 2014. The Downward Influence of Stratospheric Sudden Warmings*. *Journal of the Atmospheric Sciences*, 71(10): 3856–3876. https://doi.org/10.1175/JAS-D-14-0012.1.

Jiménez-Esteve B, Domeisen DI V. 2018. The Tropospheric Pathway of the ENSO–North Atlantic Teleconnection. *Journal of Climate*, 31(11): 4563–4584. https://doi.org/10.1175/JCLI-D-17-0716.1.

Johnson SJ, Stockdale TN, Ferranti L, Balmaseda MA, Molteni F, Magnusson L, Tietsche S, Decremer D, Weisheimer A, Balsamo G, Keeley SPE, Mogensen K, Zuo H, Monge-Sanz BM. 2019. SEAS5: The new ECMWF seasonal forecast system. *Geoscientific Model Development*. Copernicus GmbH, 12(3): 1087–1117. https://doi.org/10.5194/gmd-12-1087-2019.

Karpechko AYu, Hitchcock P, Peters DHW, Schneidereit A. 2017. Predictability of downward propagation of major sudden stratospheric warmings. *Quarterly Journal of the Royal Meteorological Society*. John Wiley & Sons, Ltd. https://doi.org/10.1002/qj.3017.

Kautz L, Polichtchouk I, Birner T, Garny H, Pinto JG. 2020. Enhanced extended-range predictability of the 2018 late-winter Eurasian cold spell due to the stratosphere. *Quarterly Journal of the Royal Meteorological Society*. John Wiley and Sons Ltd, 146(727): 1040–1055. https://doi.org/10.1002/qj.3724.

King AD, Butler AH, Jucker M, Earl NO, Rudeva I. 2019. Observed Relationships Between Sudden Stratospheric Warmings and European Climate Extremes. *Journal of Geophysical Research: Atmospheres*. Blackwell Publishing Ltd, 124(24): 13943–13961. https://doi.org/10.1029/2019JD030480.

King MP, Li C, Sobolowski S. 2021. Resampling of ENSO teleconnections: accounting for cold season evolution reduces uncertainty in the North Atlantic. *Weather and Climate Dynamics Discussions*. Copernicus GmbH, 1–24. https://doi.org/10.5194/wcd-2021-15.

Kodera K, Mukougawa H, Maury P, Ueda M, Claud C. 2016. Absorbing and reflecting sudden stratospheric warming events and their relationship with tropospheric circulation. *Journal of Geophysical Research: Atmospheres*, 121(1): 80–94. https://doi.org/10.1002/2015JD023359.

Kretschmer M, Cohen J, Matthias V, Runge J, Coumou D. 2018a. The different stratospheric influence on cold-extremes in Eurasia and North America. *npj Climate and Atmospheric Science*. Nature Publishing Group, 1(1): 44. https://doi.org/10.1038/s41612-018-0054-4.

Kretschmer M, Cohen J, Matthias V, Runge J, Coumou D. 2018b. The different stratospheric influence on cold-extremes in Eurasia and North America. *npj Climate and Atmospheric Science*, 1(1): 44. https://doi.org/10.1038/s41612-018-0054-4.

Kretschmer M, Coumou D, Agel L, Barlow M, Tziperman E, Cohen J. 2018c. More-Persistent Weak Stratospheric Polar Vortex States Linked to Cold Extremes. *Bulletin of the American Meteorological Society*, 99(1): 49–60. https://doi.org/10.1175/BAMS-D-16-0259.1.

Mariotti A, Baggett C, Barnes EA, Becker E, Butler A, Collins DC, Dirmeyer PA, Ferranti L, Johnson NC, Jones J, Kirtman BP, Lang AL, Molod A, Newman M, Robertson AW, Schubert S, Waliser DE, Albers J. 2020. Windows of Opportunity for Skillful Forecasts Subseasonal to Seasonal and Beyond. *Bulletin of the American Meteorological Society*, 101(5): E608–E625. https://doi.org/10.1175/bams-d-18-0326.1.

Matthias V, Kretschmer M. 2020. The influence of stratospheric wave reflection on North American cold spells. *Monthly Weather Review*. American Meteorological Society, 148(4): 1675–1690. https://doi.org/10.1175/MWR-D-19-0339.1.

Maycock AC, Hitchcock P. 2015. Do split and displacement sudden stratospheric warmings have different annular mode signatures? *Geophysical Research Letters*, 42(24): 10,943-10,951. https://doi.org/10.1002/2015GL066754.

Stockdale T, Johnson S, Ferranti L, Balamseda M, Briceag S. 2018. ECMWF's new long-range forecasting system SEAS5. *ECMWF Newsletter*, (154).

Tietsche S, Balmaseda M, Zuo H, Roberts C, Mayer M, Ferranti L. 2020. The importance of North Atlantic Ocean transports for seasonal forecasts. *Climate Dynamics*, 55(7): 1995–2011. https://doi.org/10.1007/s00382-020-05364-6.

Van Der Wiel K, Bloomfield HC, Lee RW, Stoop LP, Blackport R, Screen JA, Selten FM. 2019. The influence of weather regimes on European renewable energy production and demand. *Environmental Research Letters*. Institute of Physics Publishing, 14(9): 094010. https://doi.org/10.1088/1748-9326/ab38d3.

Vitart F, Robertson AW. 2018. The sub-seasonal to seasonal prediction project (S2S) and the prediction of extreme events. *npj Climate and Atmospheric Science*. Springer US, 1(1): 1–7. https://doi.org/10.1038/s41612-018-0013-0.

Waugh DW, Sobel AH, Polvani LM. 2016. What is the Polar Vortex, and how does it influence weather? *Bulletin of the American Meteorological Society*, BAMS-D-15-00212.1. https://doi.org/10.1175/BAMS-D-15-00212.1.

Weisheimer A, Palmer TN. 2014. On the reliability of seasonal climate forecasts. *Journal of The Royal Society Interface*, 11(96).

White CJ, Carlsen H, Robertson AW, Klein RJT, Lazo JK, Kumar A, Vitart F, Coughlan de Perez E, Ray AJ, Murray V, Bharwani S, MacLeod D, James R, Fleming L, Morse AP, Eggen B, Graham R, Kjellström E, Becker E, Pegion K V., Holbrook NJ, McEvoy D, Depledge M, Perkins-Kirkpatrick S, Brown TJ, Street R, Jones L, Remenyi TA, Hodgson-Johnston I, Buontempo C, Lamb R, Meinke H, Arheimer B, Zebiak SE. 2017. Potential applications of subseasonal-to-seasonal (S2S) predictions. *Meteorological Applications*, 24(3): 315–325. https://doi.org/10.1002/met.1654.

White I, Garfinkel CI, Gerber EP, Jucker M, Aquila V, Oman LD. 2019. The downward influence of sudden stratospheric warmings: Association with tropospheric precursors. *Journal of Climate*. American Meteorological Society, 32(1): 85–108. https://doi.org/10.1175/JCLI-D-18-0053.1.

Figures

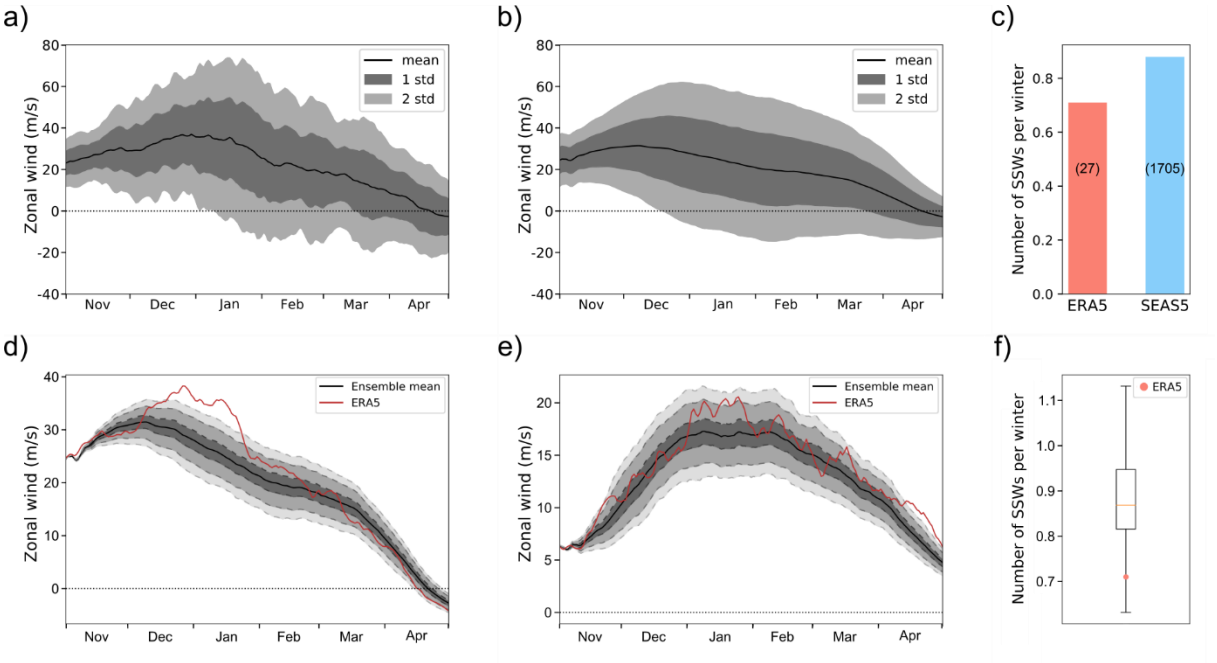

FIGURE 1. Comparison between the SPV in the observational record (ERA5) and the model dataset (SEAS5). (a) and (b) Climatology of the SPV, defined as the zonal-mean zonal wind velocity at 60°N at 10 hPa (thin black line) for ERA5 and SEAS5, respectively. The dark and light grey shadings correspond to the one and two standard deviation. (c) Number of SSWs per winter for ERA5 (red) and SEAS5 (blue). The raw number of SSWs is indicated in brackets on the bars. (d) Bootstrap estimate of sampling uncertainty associated with 38-year mean of the SPV. The bootstrap estimate was generated using 10,000 timeseries of length 38 and randomly choosing one ensemble member for each year. Dashed lines represent the 1st, 5th, 25th, 75th, 95th and 99th percentiles. The red line corresponds to ERA5 observations. (e.) Same as (d) but computing the SPV standard deviation instead of the mean. (f) Number of SSWs per winter in the 10,000 timeseries. The orange line indicates the median, the box indicates the quartiles, and the whiskers show the 5th and 95th percentiles. The red dot indicates the observational value.

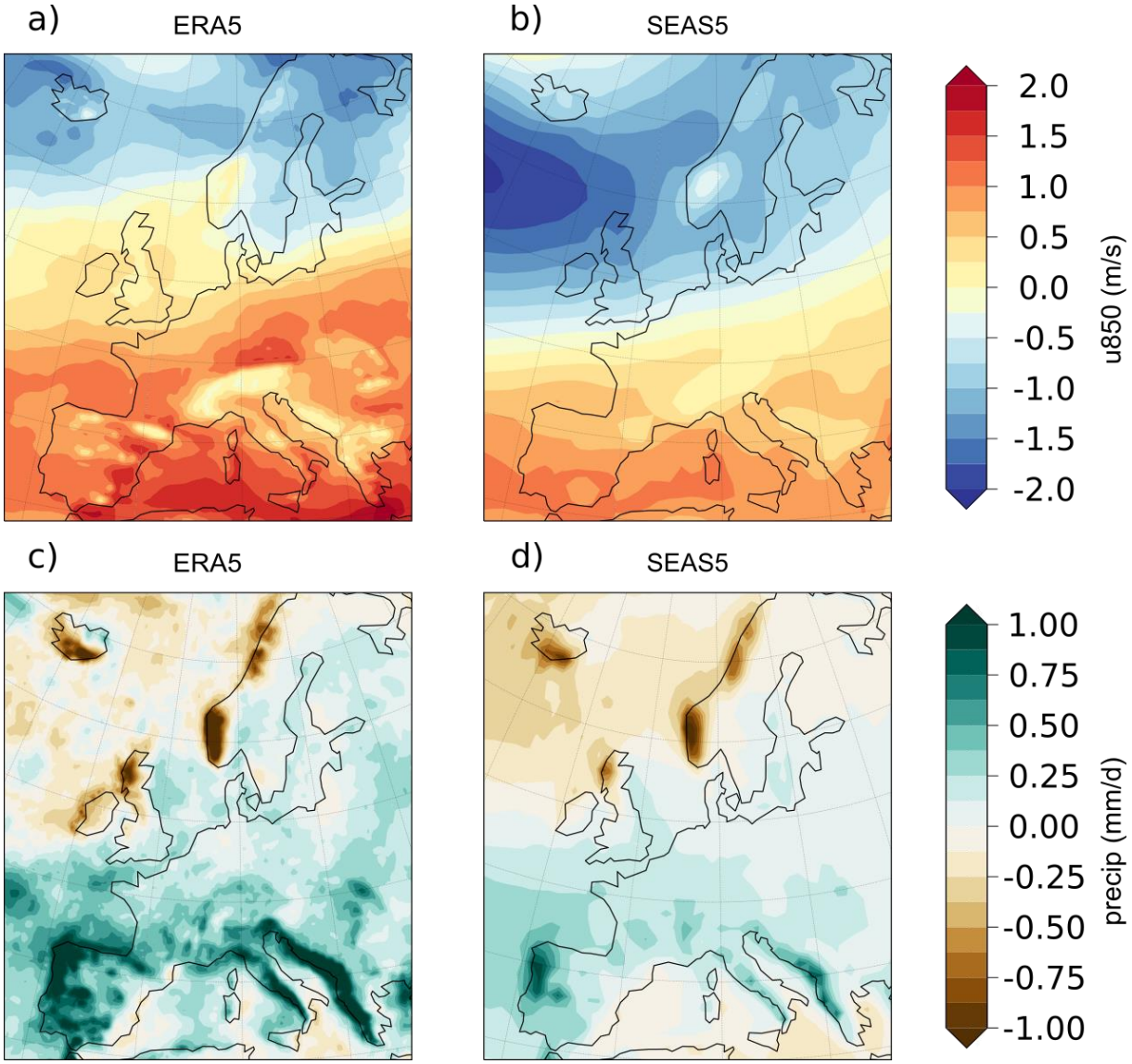

FIGURE 2. Tropospheric response to SSWS. The panels show the 30-days averages of u850 (top row) and precipitation (bottom row) anomalies after the SSW central date, averaged over all SSWs in ERA5 (panels a, c) and SEAS5 (panels b, d).

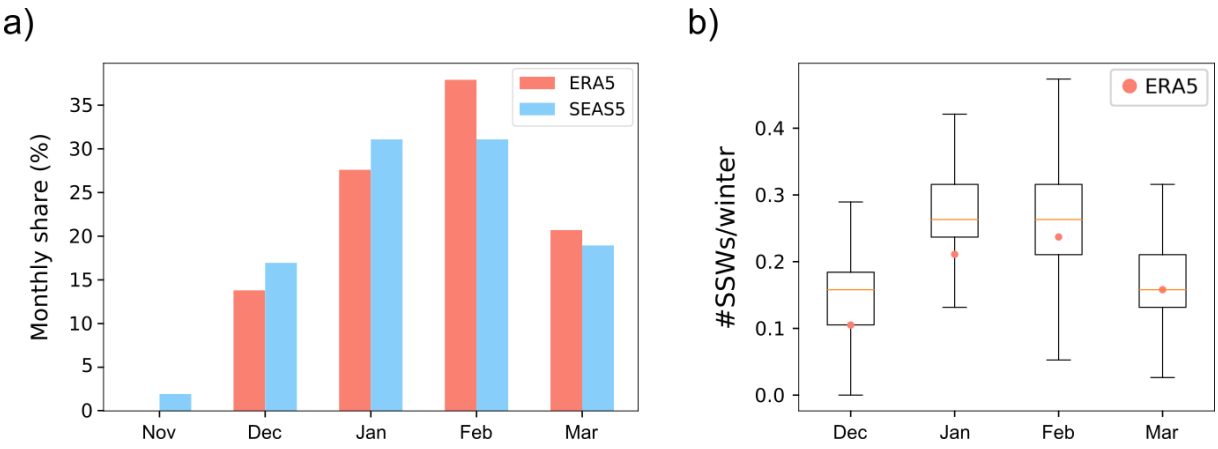

FIGURE 3. Representation of the SSW timing. (a) Number of SSWs per month, shown as a fraction of all the events for ERA5 (red) and SEAS5 (blue) for each month of the winter season. (b) Distribution of the number of SSWs per winter month, calculated for the 10,000 model timeseries. The orange lines indicate the median, the boxes indicate the quartiles, and the whiskers show the 5th and 95th percentiles. The red dots are the observed values.

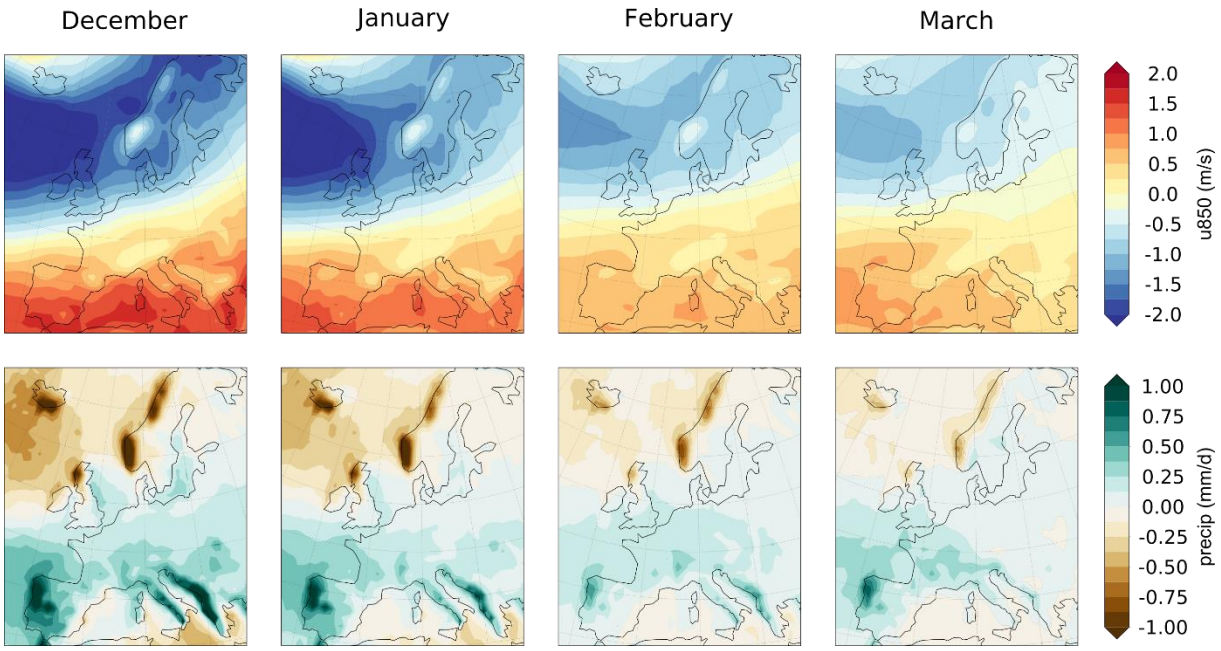

FIGURE 4. Tropospheric response to SSWs split by month. 30-days averages of u850 (top row) and precipitation (bottom row) anomalies after the SSW central date for each month in the winter season for SEAS5.

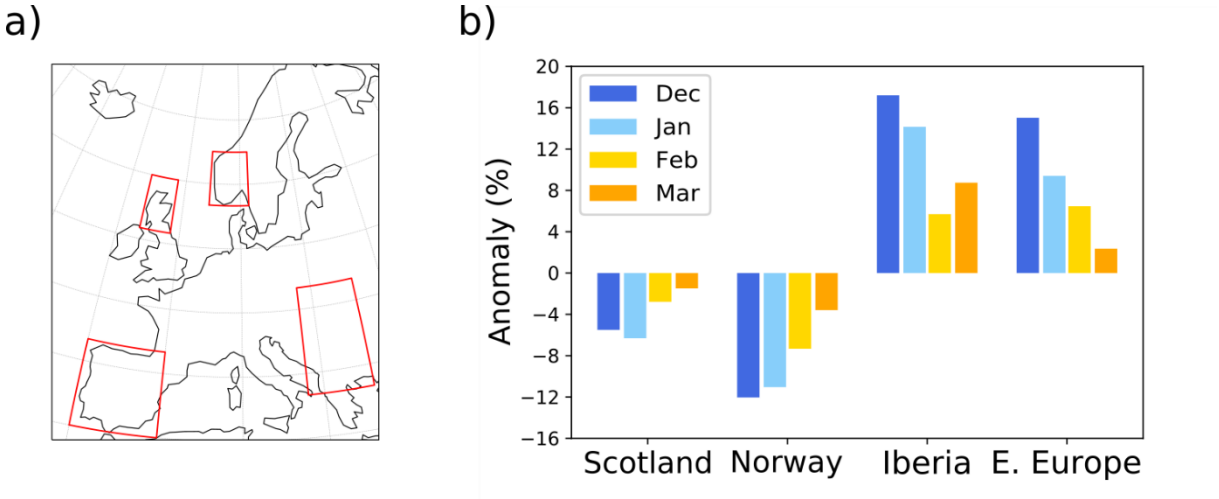

FIGURE 5. Regional precipitation anomalies. (a) Map of Europe showing the four regions (red rectangles) over which regional indices are calculated: Scotland (6.5-1.5 °W, 55-60°N), Norway (4.5-11.5 °E, 58-63°N), Iberia (10°W-1°E, 36-44°N), Eastern Europe (18-26 °E, 40-50°N). (b) 30-days averaged precipitation anomalies following SSWs normalized by the multi-year monthly climatology, for each region and each month of the winter season.

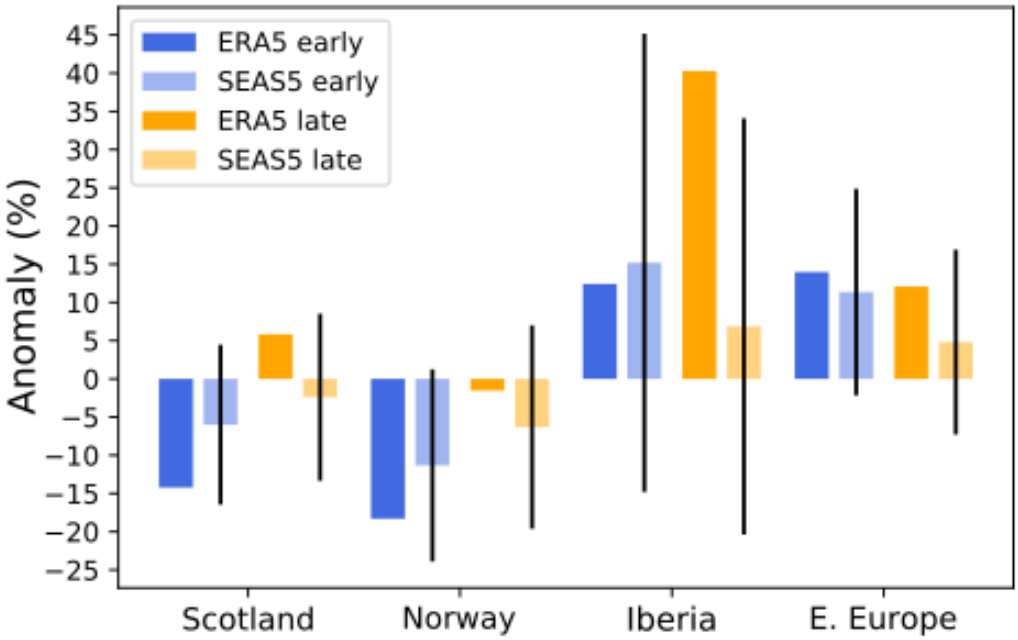

FIGURE 6. Consistency with the observations and the role of sampling uncertainty. 30-days averaged precipitation anomalies following SSWs normalized by the multi-year early (DJ) and late winter (FM) climatology, for each region and split by early or late winter occurrence. The observations are shown by the dark blue and yellow bars. The light blue and orange bars show the results for the model, with the height of the bars indicating the median of the 10,000 timeseries (see methods) and the black lines indicating the 5th and 95th percentile.

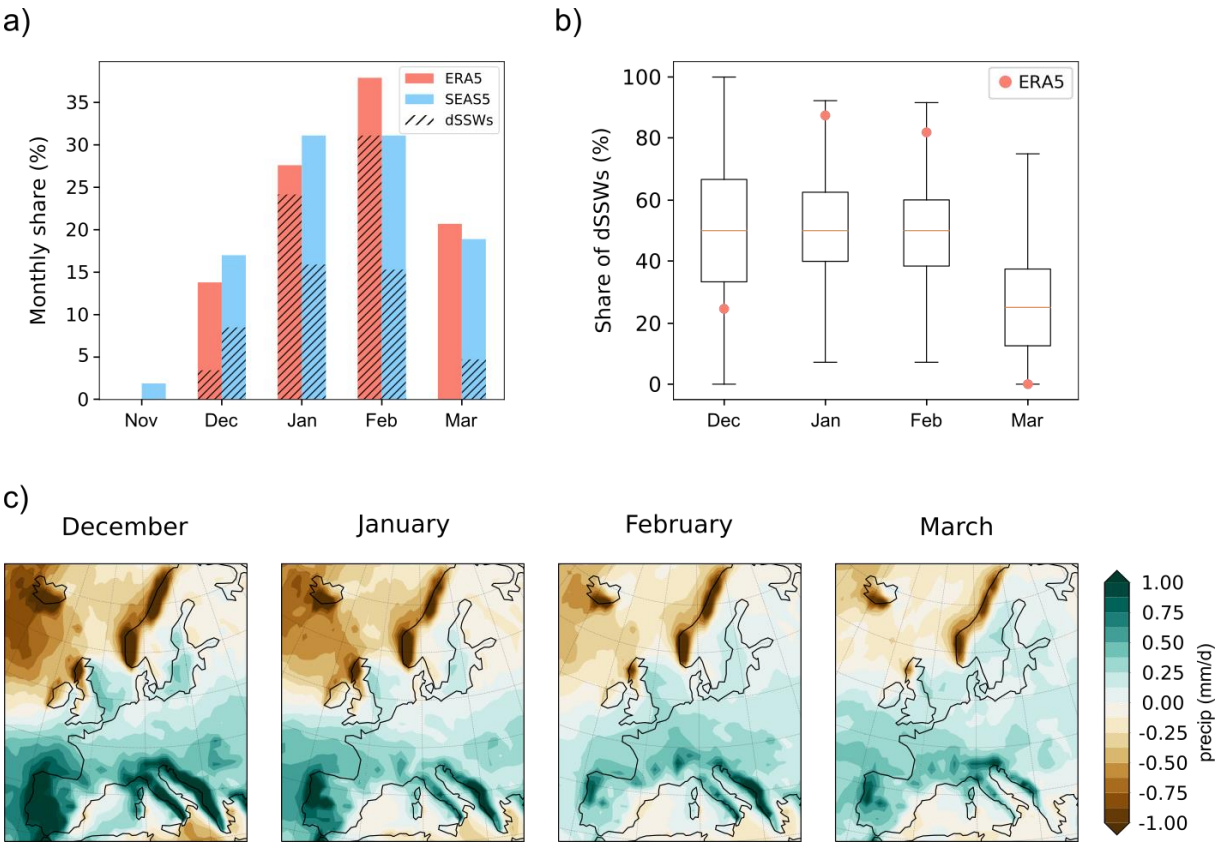

FIGURE 7. The role of downward propagation of SSWs (dSSWs). (a) Proportion of dSSWs per month (dashed) for ERA5 (red) and SEAS5 (blue) for each month in winter. (b) Share of dSSWs of all SSWs per month in the 10,000 model timeseries. Orange lines are the medians over all timeseries. Red dots are the observed values. The whiskers indicate the 5th and 95th percentiles. (c) Same as in Fig. 4b but only for dSSWs.

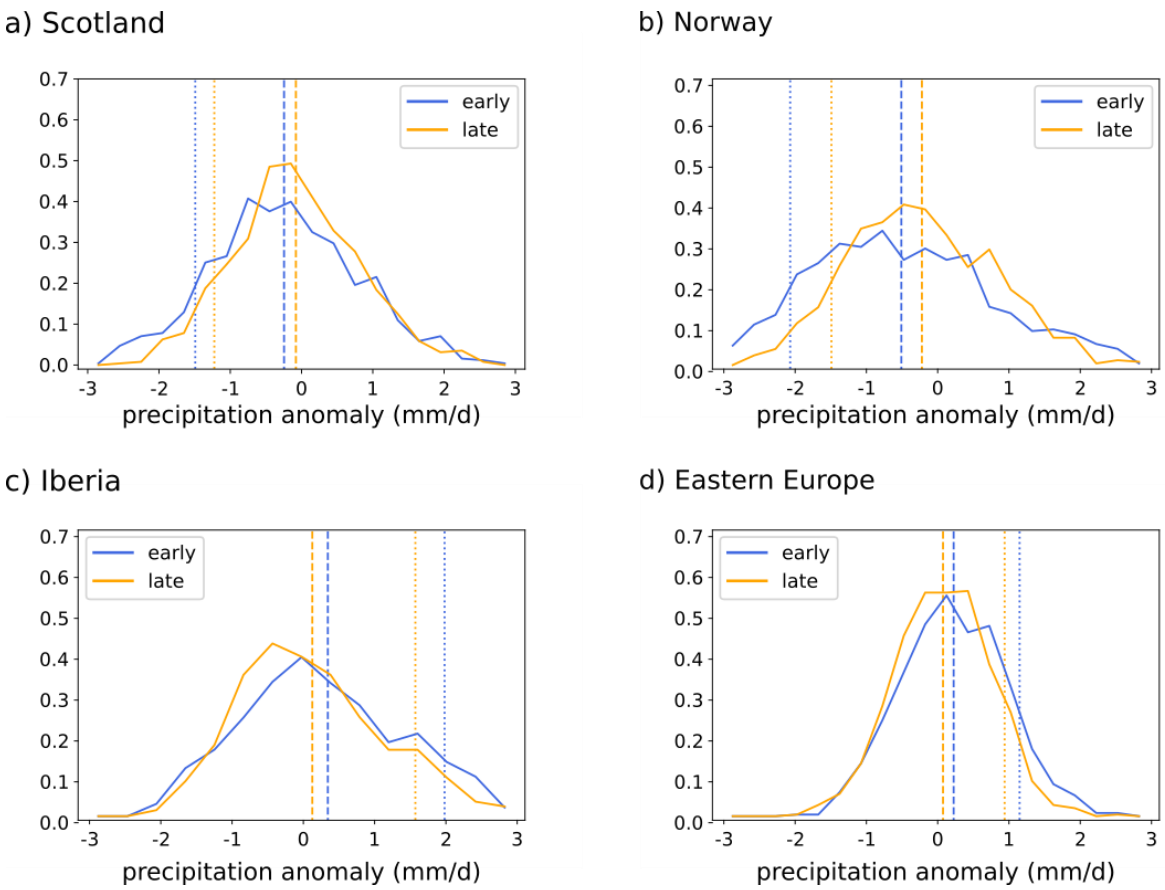

FIGURE 8. Probability density functions of 30-days averaged precipitation anomalies following early winter SSWs (blue) and late winter SSWs (orange) for (a) Scotland [6.5-1.5°W, 55-60°N], (b) Norway [4.5-11.5°E, 58-63°N], (c) Iberia [-10°W to 1°E, 36-44°N] and (d) Eastern Europe [18-26°E, 40-50°N]. The dashed lines show the average precipitation anomalies and the dotted lines show the 10th (a,b) and 90th (c,d) percentiles.